3-1-2008

Seasonal Variability of the Observed Barrier Layer in the Arabian Sea

Pankajakshan Thadathil
National Institute of Oceanography

Prasad Thoppil
University of Southern Mississippi

R.R. Pao
Naval Physical Oceanographic Laboratory

P.M. Muraleedharan
National Institute of Oceanography

Y.K. Somayajulu
National Institute of Oceanography

See next page for additional authors

Seasonal Variability of the Observed Barrier Layer in the Arabian Sea*

PANKAJAKSHAN THADATHIL,[+] PRASAD THOPPIL,[#] R. R. RAO,[@] P. M. MURALEEDHARAN,[+] Y. K. SOMAYAJULU,[+] V. V. GOPALAKRISHNA,[+] RAGHU MURTUGUDDE, [&] G. V. REDDY,[+] AND C. REVICHANDRAN[**]

[+] *National Institute of Oceanography, Dona Paula, Goa, India*
[#] *Department of Marine Science, University of Southern Mississippi, Hattiesburg, and NASA Stennis Space Center, Stennis Space Center, Mississippi*
[@] *Naval Physical Oceanographic Laboratory, Kochi, India*
[&] *Earth Sciences Interdisciplinary Center, University of Maryland, College Park, College Park, Maryland*
[**] *National Institute of Oceanography Regional Centre, Kochi, India*

(Manuscript received 12 March 2007, in final form 1 August 2007)

ABSTRACT

The formation mechanisms of the barrier layer (BL) and its seasonal variability in the Arabian Sea (AS) are studied using a comprehensive dataset of temperature and salinity profiles from Argo and other archives for the AS. Relatively thick BL of 20–60 m with large spatial extent is found in the central-southwestern AS (CSWAS), the convergence zone of the monsoon wind, during the peak summer monsoon (July–August) and in the southeastern AS (SEAS) and northeastern AS (NEAS) during the winter (January–February). Although the BL in the SEAS has been reported before, the observed thick BL in the central-southwestern AS during the peak summer monsoon and in the northeastern AS during late winter are the new findings of this study. The seasonal variability of BL thickness (BLT) is closely related to the processes that occur during summer and winter monsoons. During both seasons, the Ekman processes and the distribution of low-salinity waters in the surface layer show a dominant influence on the observed BLT distributions. In addition, Kelvin and Rossby waves also modulate the observed BL thickness in the AS. The relatively low salinity surface water overlying the Arabian Sea high-salinity water (ASHSW) provides an ideal ground for strong haline stratification in the CSWAS (during summer monsoon) and in NEAS (during winter monsoon). During summer, northward advection of equatorial low-salinity water by the Somali Current and the offshore advection of low-salinity water from the upwelling region facilitate the salinity stratification that is necessary to develop the observed BL in the CSWAS. In the SEAS, during winter, the winter monsoon current (WMC) carries less saline water over relatively high salinity ambient water to form the observed BL there. The winter West India Coastal Current (WICC) transports the low-salinity water from the SEAS to the NEAS, where it lies over the subducted ASHSW leading to strong haline stratification. Ekman pumping together with the downwelling Kelvin wave in the NEAS deepen the thermocline to cause the observed thick BL in the NEAS.

1. Introduction

The role of haline stratification in limiting the mixed layer depth (MLD) and in the development of an intermediate layer called the barrier layer (hereinafter referred to as BL) between the MLD and the top of the thermocline was first reported in the Pacific by Lukas and Lindstrom (1991). The difference between the isothermal layer depth (ILD) and MLD is defined as the BL thickness. The BL inhibits entrainment cooling of the mixed layer by preventing the exchange of heat with cooler subsurface layers and thus plays a significant role in the evolution of sea surface temperatures (SSTs). The BL acts as a "barrier" for the transfer of heat, momentum, mass, and nutrient fluxes between the mixed layer and the thermocline. The Tropical Ocean Global Atmosphere (TOGA) Coupled Ocean–Atmosphere Response Experiment (COARE) has shown the robustness of the BL in decreasing the en-

* NIO Contribution Number 4277.

Corresponding author address: Pankajakshan Thadathil, National Institute of Oceanography, Dona Paula, Goa, India.
E-mail: pankaj@nio.org

DOI: 10.1175/2007JPO3798.1

trainment cooling in the western Pacific warm pool (Tomczak 1995; You 1995; Ando and Mc Phaden 1997; Vialard and Delecluse 1998a,b). Vialard and Delecluse (1998a) reported the complex impact of the BL on SST. In regions of a very shallow mixed layer (ML), the BL traps a significant part of the penetrating solar radiation, leading to temperature inversions (Jerlov 1968; Lewis et al. 1990; Anderson et al. 1996). Further, in the presence of the BL, the oceanic response to wind forcing also increases (Vialard and Delecluse 1998a) by trapping momentum in the ML. Weakening of the BL off Sumatra was identified to be an important process that reinforces the oceanic anomalies favoring the strengthening of air–sea interaction during the Indian Ocean dipole/zonal mode (IODZM) events (Murtugudde et al. 2000; Murtugudde and Busalacchi 1999; Masson et al. 2002). All of the above findings show the importance of BL in regulating ocean–atmosphere interactions, which in turn affect weather and climate.

The main candidate that forces BL is the presence of a halocline in the surface layer. The halocline in the surface layer occurs when the surface salinity is reduced significantly, compared to the subsurface layer by processes such as excess precipitation over evaporation, river runoff, and redistribution of the low-salinity water by horizontal advection. These low-salinity water fluxes can act in concert, as in the Bay of Bengal (Thadathil et al. 2007), or individually, as, for example, in the western Pacific, where high precipitation is accompanied by westerly wind bursts, the former (latter) favoring a shallow (deeper) ML (Anderson et al. 1996).

In the northern Indian Ocean, besides the Bay of Bengal (BOB), there are also regions of strong haline stratification that are conducive to the formation of a thick BL. Figure 1 shows a comparison of profiles with haline stratification from representative regions in the northern Indian Ocean. Although Sprintall and Tomczak (1992) and Rao and Sivakumar (2003) discussed the BL formation in the Indian Ocean, these studies were based on sparse datasets. On a regional scale, a few studies exist for the BOB and the southeastern tropical Indian Ocean. Masson et al. (2002) performed the same analysis as Sprintall and Tomczak (1992) using the monthly climatology of Levitus (1998) and reported a thick (40 m) and robust BL in the BOB during November–March with maximum spatial extent in February. Using time series measurements made from a stationary location (18.5°N, 89°E) in the northern BOB, Vinayachandran et al. (2002) have described the observed intraseasonal evolution of BL during the summer monsoon of 1999. Using the Argo and other hydrographic data, Thadathil et al. (2007) provided a comprehensive analysis of the BL formation and its seasonal variability in the BOB. In another comprehensive study using hydrographic data archives, Qu and Meyers (2005) studied the formation mechanisms and seasonal variation of BL in the southeastern tropical Indian Ocean (SETIO). They reported a thick BL (~40 m) to the west of Sumatra.

As shown in Fig. 1, there are three regions in the Arabian Sea (AS) where the haline stratification near the surface is strong and favorable for the formation of a thick BL. Shenoi et al. (2004) studied the observed decaying phase of the BL in the southeastern AS (SEAS). Durand et al. (2007) simulated the BL in this region qualitatively.

A comprehensive study on the BL formation and its seasonal variability in the three regions (2, 3, and 4 shown in Fig. 1) in the AS has been lacking due to the paucity of data. Significant reduction in surface salinity ($E - P$, runoff, and circulation) need not always be the cause for haline stratification and BL formation. Subduction of high-salinity water underneath a marginally low salinity surface water may also induce the required haline stratification in the surface layer to form a BL as seen in the regions 4 and 5 shown in Fig. 1. The BL formation in the northeastern AS (NEAS) and central-southwestern AS (CSWAS) (addressed in this study), is caused by such subduction of high-salinity water. The transport of surface low-salinity water from the equator to the southwestern and central AS by the Somali Current during summer monsoon and the existence of Arabian Sea high-salinity water (ASHSW) in the subsurface layer (Rochford 1964; Shenoi et al. 1993; Morrison 1997; Kumar and Prasad 1999; Prasad and Ikeda 2002a,b; Joseph and Freeland 2005) lead to a strong haline stratification. During winter, the poleward flowing West India Coastal Current (WICC; Shetye et al. 1991; McCreary et al. 1993) carries the relatively fresh water from the BOB to the northeastern AS and sits over the subsurface ASHSW.

One of the salient features of the BL formation in the northern Indian Ocean during winter is the presence of temperature inversion within the BL [Thadathil and Gosh 1992 (SEAS); Thadathil et al. 2002; Thadathil et al. 2007 (BOB); Qu and Meyers 2005 (SETIO); Durand et al. 2004; and Shenoi et al. 2004 (SEAS)]. Doe (1965) and Banse (1968) reported surface layer temperature inversion in the NEAS caused by strong haline stratification. Thadathil et al. (2007) proposed a new method to compute the BL in the regions of temperature inversion. Since the method of Thadathil et al. represents the BL more realistically, the same methodology is used in this study to describe the BL in the entire basin.

The deployment of Argo profiling floats in the AS has generated a novel dataset that is ideal for BL com-

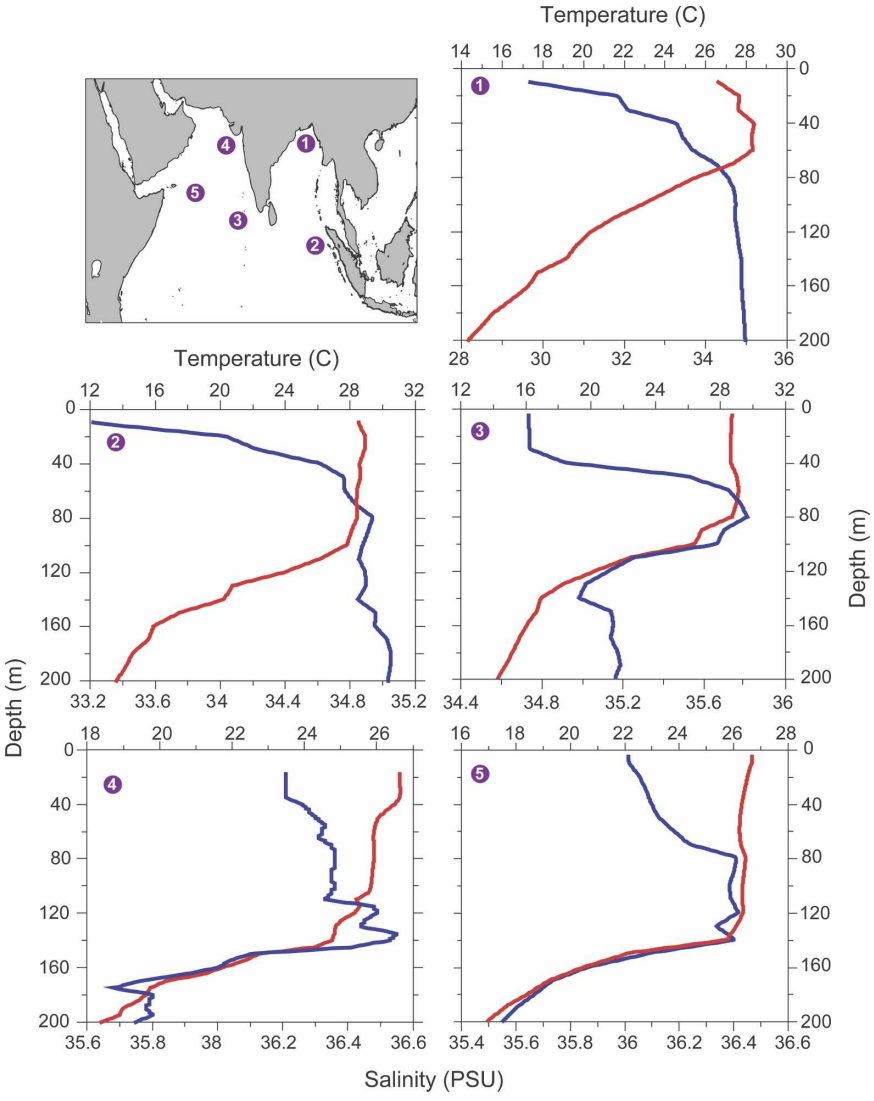

FIG. 1. Regions of significant haline stratification in the Indian Ocean. Region 1: northern Bay of Bengal, Region 2: eastern south-equatorial Indian Ocean, Region 3: southeastern Arabian Sea, Region 4: central southwestern Arabian Sea, and Region 5: northeastern Arabian Sea. The red and blue curves show temperature (T) and salinity (S), respectively.

putations along with hydrographic data collected in the AS under the national programs, archived in the Indian Oceanographic Data Centre (IODC). The *World Ocean Atlas 1998* (*WOA-98*) and the updated *WOA-2001* consist of only limited data from the IODC archive. Therefore, the combination of these data from three different sources (*WOA-2001*, IODC, and Argo) facilitates a comprehensive dataset for the AS to resolve the BL structure and its variability. In this study, we examine the BL formation and its variability using this comprehensive dataset. The rest of the paper is organized as follows: Section 2 describes the data and methodology used in the study. The seasonal variability of BL thickness (BLT), ILD, and MLD are presented in section 3. In section 4 the formation mechanism of the BL is examined, which is followed by a summary and conclusions in section 5.

2. Data and methodology

The spatial distribution of data used in the present study is shown in Fig. 2. Figure 2a represents the station coverage of profiles from Argo floats. Under the international Argo project, Argo profiling floats are deployed in the AS by national and international agencies. High-quality temperature and salinity profiles

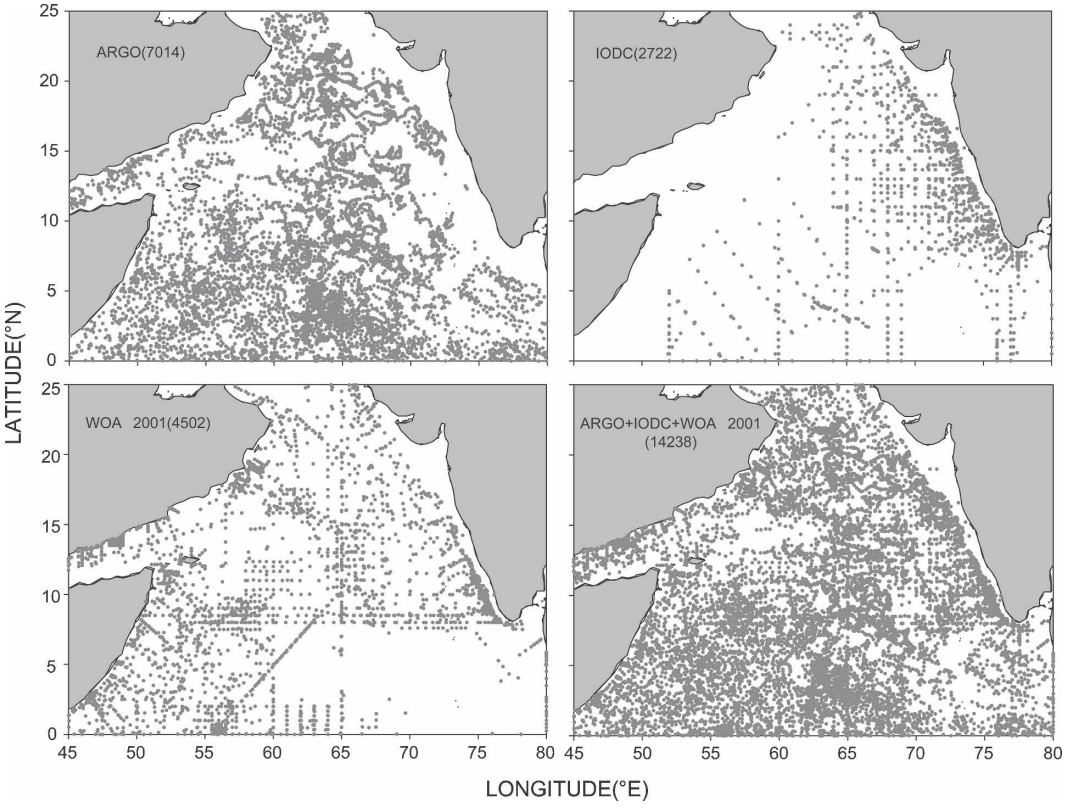

FIG. 2. Geographical distribution of hydrographic (temperature and salinity) stations in the Arabian Sea considered in the present study: (a) Argo profiling floats, (b) IODC, (c) *WOA-2001*, and (d) all three sources (Argo + IODC + *WOA-2001*). The number of stations within each category is given in parentheses in the respective panels.

from the floats generated during December 2001–October 2006 are used in the present study. The Argo depth resolution is about 10 m down to 100 m and, therefore, should resolve the BL in the AS with resolution ~10 m. The expected accuracies of temperature and salinity from the floats are 0.005°C and 0.01 psu, respectively (Argo Science Team 2000). Though the Argo data have been subjected to real-time quality check, the data used in the present study have been subjected to additional quality check using "float-to-float" and "float-to-ship" CTD validations as reported by Thadathil and Muraleedharan (2004) and Thadathil et al. (2007). The data were linearly interpolated at 1-m intervals.

The spatial coverage of hydrographic data from the IODC archive is shown in Fig. 2b. Figure 2c represents the *WOA-2001* station coverage in the AS for selected hydrographic data (bottle and CTD) with "good" quality flags. While selecting the data from *WOA-2001* and IODC databases, duplicate profiles from both archives are removed. In the case of bottle data, if a particular station does not have data at all standard depths up to 100 m, the stations are not considered for the present study. If data at any standard depth above 100 m is missing, it results in inaccurate representation of the BL. In all cases, profiles shallower than 100 m are not considered for analysis. Figure 2d represents the spatial coverage of total stations from all three sources. Seasonal distributions of number of profiles in each $1° \times 1°$ grid box from the combined data are provided in Fig. 3. While the data coverage is satisfactory for the summer monsoon, the northeastern AS shows sparse coverage for the winter monsoon. The uncertainty involved in objective mapping of the variables to this data-sparse region is discussed in section 3.

We computed ILD and MLD from individual profiles. The MLD is defined as the depth at which

$$\sigma_{t[z=h]} = \sigma_{t[z=0]} + \Delta T \frac{d\sigma_t}{dT}, \tag{1}$$

where $\sigma_{t(z=0)}$ is the surface σ_t value, ΔT the desired temperature criterion [1°C, following Wyrtki (1971)], and $d\sigma_t/dT$ is the coefficient of thermal expansion

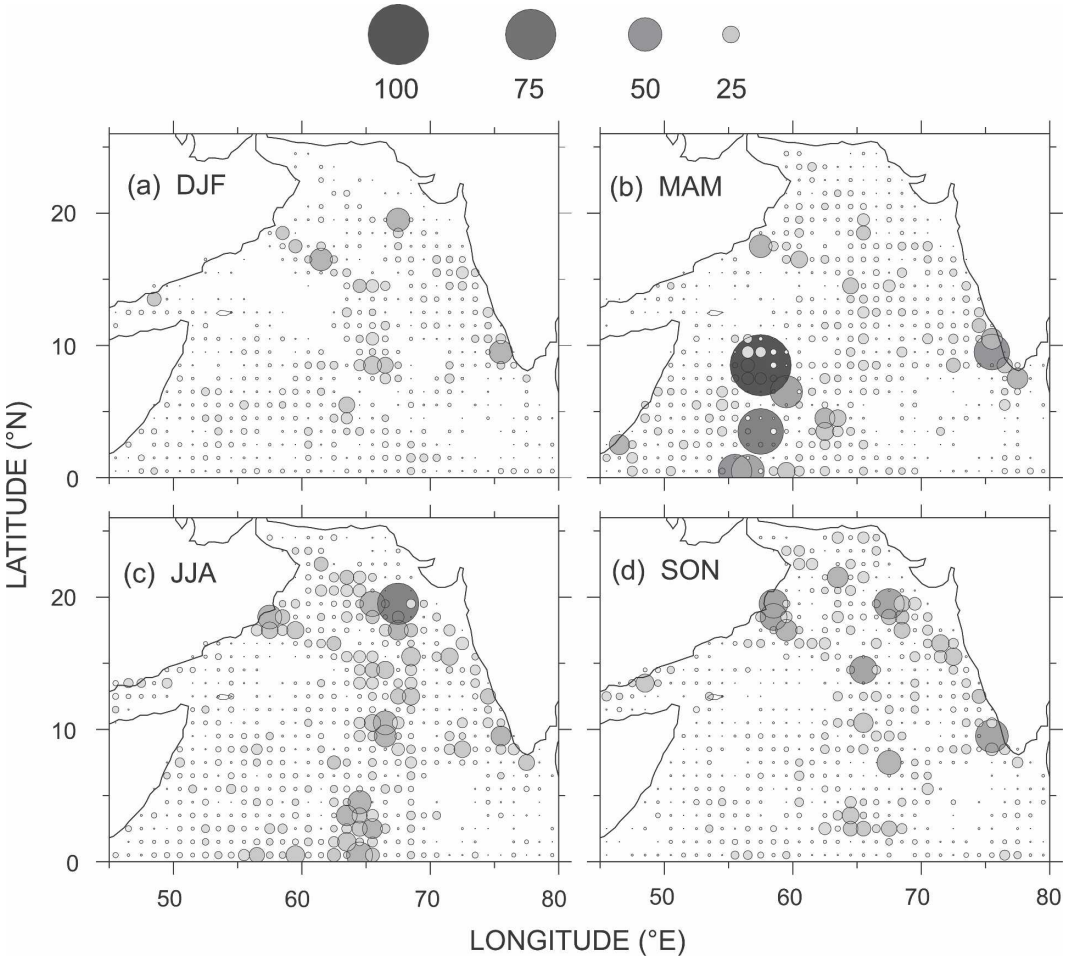

FIG. 3. Seasonal distribution of number of profiles in 1° × 1° bins from the combined product (a) December–February, (b) March–May, (c) June–August, and (d) September–November. Radius and shading of the circles indicate the number of profiles.

evaluated using the surface temperature and salinity (Sprintall and Tomczak 1992; Kara et al. 2000; Rao and Sivakumar 2003). The ILD, the depth up to the top of the thermocline, is defined as the depth at which temperature decreases by 1°C from SST (Sprintall and Tomczak 1992; Kara et al. 2000; Rao and Sivakumar 2003). The above definition of ILD holds well for normal temperature profiles without any temperature inversion in the surface layer (Thadathil et al. 2007), but not during winter, when the SEAS experiences large-scale temperature inversions near the surface (Thadathil and Ghosh 1992; Gopalakrishna et al. 2005; Shankar et al. 2002; Durand et al. 2004) and the BL also attains its maximum thickness and horizontal extent. The seasonal variability of temperature inversion calculated from a comprehensive dataset of XBT and MBT is shown in Fig. 4 with the stations shown in the background. Therefore, in this study, for profiles with temperature inversions, ILD is derived using the definition of Thadathil et al. (2007). Here, ILD is defined as the depth at which the temperature at the *base of the inversion layer* is equal to the temperature at the *top of the inversion layer*. After computing MLD, ILD, and BLT, monthly scattered data of all parameters have been objectively mapped to a common grid (1° × 1°) using the kriging method (Deutsch and Journel 1992; Cressie 1991).

3. Seasonal variation of BLT

The seasonal evolution of BLT in the AS (Fig. 5) shows large variability with a rich spatial structure. During the premonsoon months of April–May, the AS is free of BL. The BL sets in with the onset of summer monsoon (June) in the southwestern AS. With the progress of the season, it builds up both in thickness

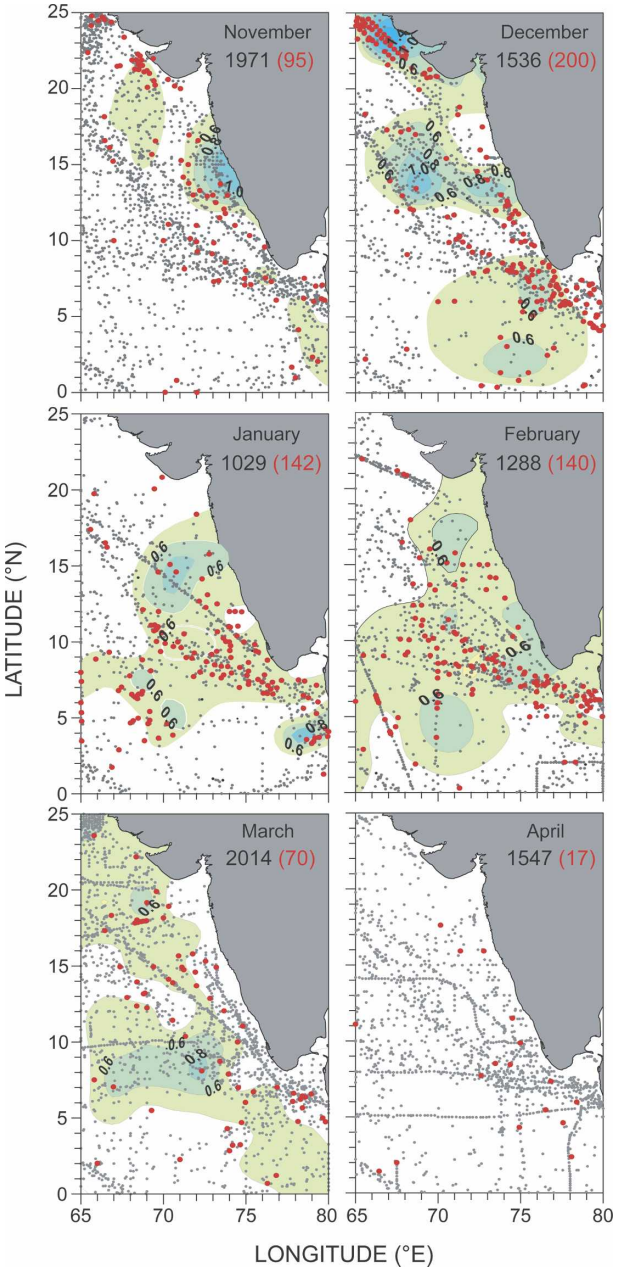

FIG. 4. Surface layer temperature inversion in the Arabian Sea derived from XBT and MBT data archived in the IODC. The red dots show locations of inversion and the black dots indicate station locations (MBT and XBT). Inversions greater than 0.2°C are contoured at interval 0.2°C.

and spatial extent, reaching the peak during August and decaying with the withdrawal of the summer monsoon during September–October. A thick BL (20–60 m) is found in the central AS, southeast of the Findlater jet and almost covers the southern AS except the SEAS. During winter, the distribution of BLT shows a distinctly different pattern from that of the summer monsoon. By November, the BL in the CSWAS vanishes completely and a thin BL (~20 m) appears in the SEAS. The BL in SEAS grows in strength and extent by December and propagates northward hugging the west coast of India in January. By February, a large area of 20–60-m thick BL is formed along the entire west coast of India with the thicker BL adjoining the coastline. The thick BL shows more offshore extent in the SEAS compared to the BL in the northeastern basin. In February, the thickness of the northward extent of the BL increases and the BL exhibits westward spreading, covering almost the entire northern AS. By March the BL begins to decay and disappears by April. Although the distribution of the winter monsoon BL in the northeastern AS (shown in broken white contours in Fig. 5) is mapped based on sparse data, the presence of strong temperature inversion (derived from spatially well represented XBT and MBT data) in the northeastern AS during winter (Fig. 4) justifies the objectively mapped thick BL shown in this region during winter.

4. Forcing mechanisms

In the AS, the surface layer is forced by local winds during the summer and winter monsoons. Since it is confined to low latitudes, propagating waves (coastally trapped Kelvin waves and associated Rossby waves) also force the surface layer of the basin remotely. The local winds, besides causing zones of divergence and convergence in the basin, also control the SST through turbulent vertical mixing and air–sea heat fluxes (Bauer et al. 1991). While Ekman pumping, propagating long waves, and net surface heating cause variability in the ILD, turbulent fluxes of heat, freshwater, and momentum across the air–sea interface and horizontal advection in the surface layer cause variability in MLD. When the MLD is determined by thermal stratification caused by net surface heat flux alone (weak wind speed regimes), both MLD and ILD will be nearly equal, resulting in a BLT minimum. Wind stresses tend to oppose the formation of BL by increasing surface turbulent kinetic energy and deepening the ML. Therefore, the main candidate that facilitates a thick BL is the freshwater flux ($E - P + R$) and its redistribution by horizontal advection (Ekman and geostrophic) in the surface layer. Since the freshwater flux and its redistribution by horizontal advection have a direct influence on the sea surface salinity (SSS), throughout this study the SSS is used as a proxy for the freshwater flux. Considering the above aspects, the processes involved in the observed BL formation are examined in light of the

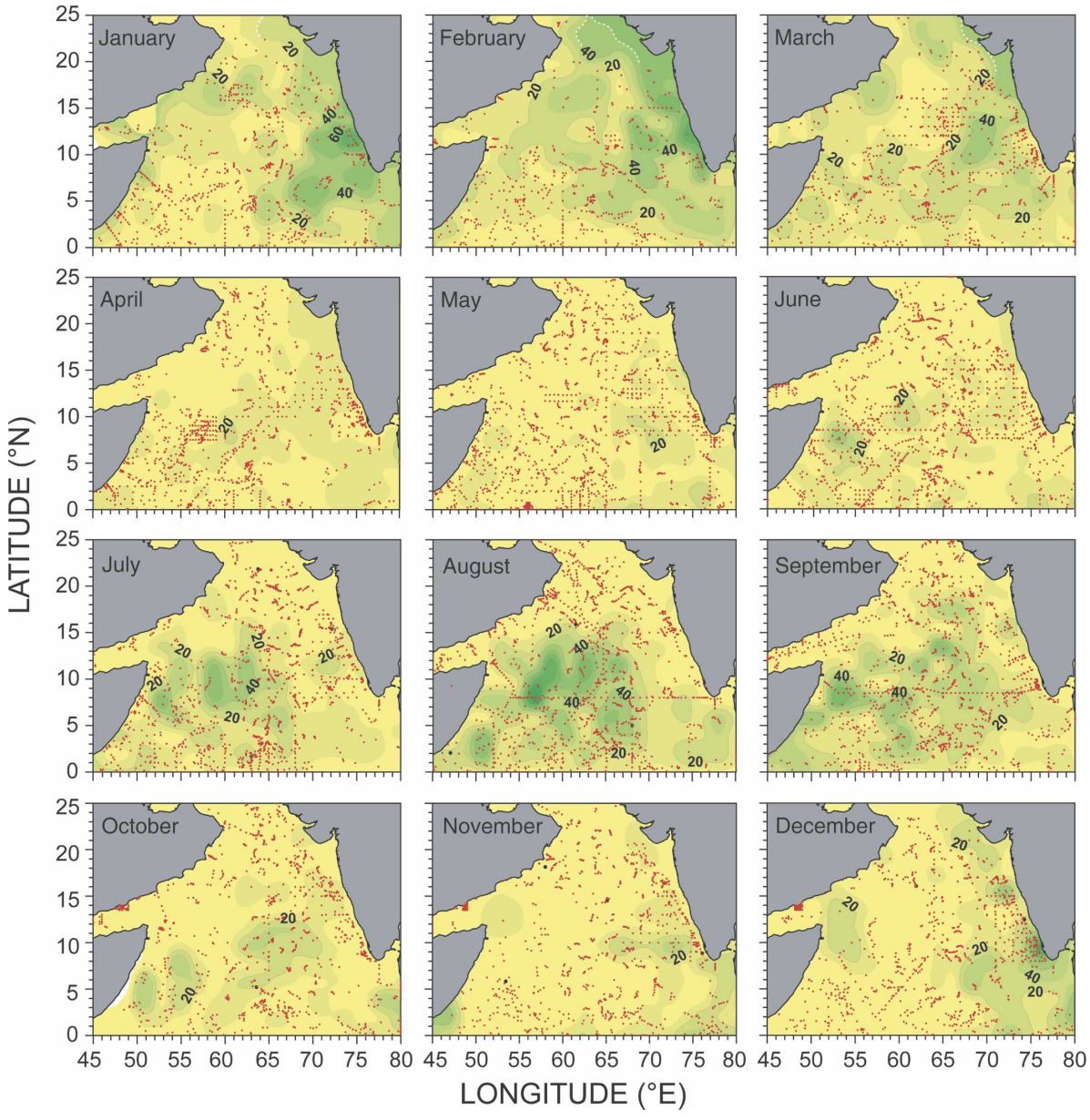

FIG. 5. Annual distribution of barrier layer thickness (m). Contour interval is 10 m, labeled at 20-m intervals.

formation mechanism(s) and variability of MLD and ILD for the summer and winter monsoon seasons.

a. Summer monsoon

During the summer monsoon, the surface circulation in the AS is dominated by Ekman drift driven by the southwesterly winds (Cutler and Swallow 1984; Shankar et al. 2002; McCreary et al. 1993; Schott and McCreary 2001) as shown in Fig. 6. While Fig. 6c shows the surface Ekman currents (Pond and Pickard 1983) for July, Fig. 6d shows the total surface currents (sum of Ekman and geostrophic currents) for the same month. For computing the surface Ekman drift the Quick Scatterometer (QuikSCAT) winds are used. Geostrophic currents are computed from the Aviso gridded product of merged *European Remote Sensing Satellite-1/2* (*ERS-1/2*) and *Jason-1* sea level anomaly (SLA) weekly global datasets during September 2001–May 2007 distributed on a ⅓° Mercator grid using the method of Chelton et al. (2003). One of the prominent processes in the basin during the summer monsoon is the development of a divergence zone northwest of the Findlater jet (Findlater 1969) and a convergence zone southeast of it (Bauer et al. 1991). Figure 7 shows wind stress curl

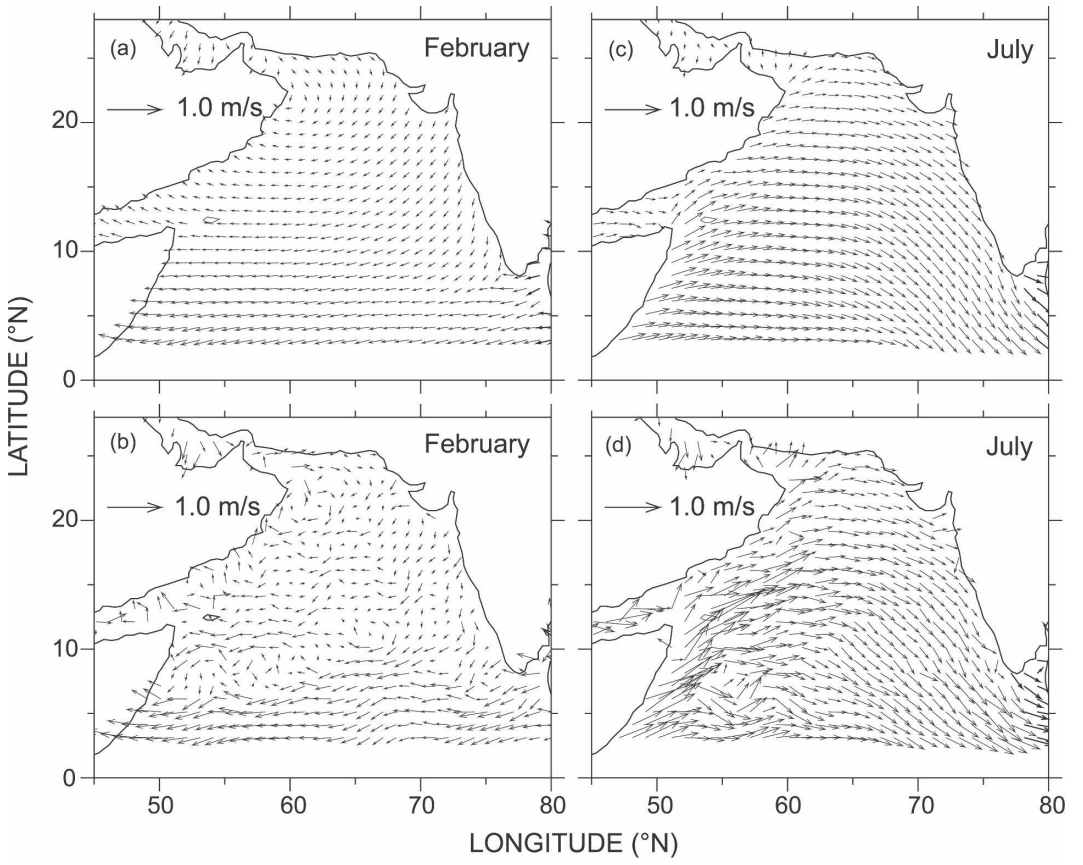

FIG. 6. Ekman surface current (m s^{-1}) and total surface current (m s^{-1}) for (a), (b) February and (c), (d) July. Total surface current is the sum of Ekman and geostrophic currents. Ekman current is computed from the QuikSCAT winds during July 1999–May 2006. Geostrophic currents are computed from gridded product of merged *ERS-1/2* and *Jason-1* sea level anomaly weekly global datasets (produced by Ssalto/Ducacs and distributed by Aviso) during September 2001–May 2007 distributed on a ⅓° Mercator grid.

(QuikSCAT winds are used owing to their better spatial resolution) in the basin for winter (February; Fig. 7a) and summer (July; Fig. 7b). During the summer monsoon (Fig. 7b), the negative and positive wind stress curls demarcate the divergence and convergence zones in the basin respectively. In the region of Ekman divergence, the effect of turbulent mixing by strong monsoon winds in deepening the MLD/ILD is opposed by the shoaling of isotherms due to suction. In contrast, the Ekman pumping in the convergence zone promotes the MLD/ILD deepening along with the turbulent vertical mixing by strong winds. The manifestation of these processes can be seen in the distribution of both MLD and ILD in Figs. 8 and 9, respectively. During April–May, throughout the basin the MLD is found to be thin (20–40 m). This is due to weak wind-driven mixing and higher net heat gain by the ocean surface.

The onset of southwest monsoon winds in June causes shoaling of the MLD along the coastal regions of the basin and deepens it in the interior, especially in the central southwestern basin. The shallow MLD in the coastal regions and deeper MLD in the open ocean continue until September. During this time, the CSWAS is characterized by relatively low salinity water. The Somali Current carries low-salinity water from the equatorial region, and the low-salinity water is also advected to the CSWAS from the Somalia upwelling regions (Bauer et al. 1991; Morrison 1997; Joseph and Freeland 2005) as is evident from the distribution of surface salinity during summer (Fig. 10). This low-salinity water is trapped over the ASHSW, which spreads along the eastern AS toward the equator, the core of which can be seen at 100 m (Fig. 1, region 5). After the formation of ASHSW in the northern AS during winter (Rochford 1964; Shenoi et al. 1993; Kumar and Prasad 1999; Prasad and Ikeda 2002a,b), it subducts to deeper layers (~100 m) as it spreads toward the equator along the 24-σ_t surface (Rochford 1964; Shenoi et al. 1993; Morrison 1997; Kumar and Prasad 1999; Prasad and Ikeda 2002a,b; Joseph and Freeland

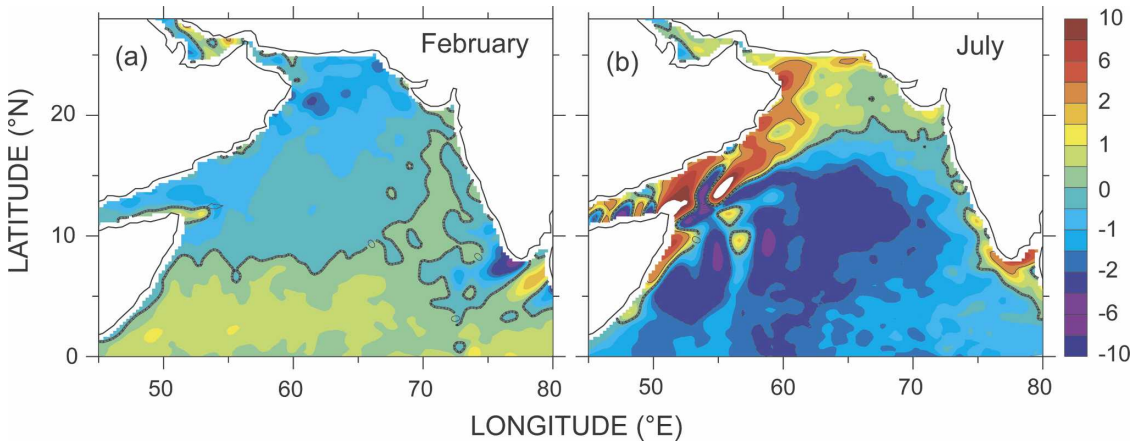

FIG. 7. Wind stress curl ($\times 10^{-7}$ N m^{-3}) for (a) February and (b) July computed using the QuikSCAT winds during July 1999–May 2006. Shading interval is 1.0 between [−10, 10] (ftp://ftp.ssmi.com/qscat).

2005). The subduction of ASHSW takes place during winter in the region north of 15°N (Prasad and Ikeda 2002a,b). During July, the Ekman convergence in the CSWAS (Fig. 7b) drives a deep ILD of 100–120 m (Fig. 9).

Thus, the limiting of the MLD due to high saline stratification, caused by the subducted ASHSW, and deepening of the ILD, due to the Ekman convergence associated with negative wind stress curl, facilitate formation of the observed thick BL in this region during July–September. Although the monsoon forcings are conducive for a thick BL, the observed reduction in BLT during September could be due to the arrival of upwelling Rossby waves in the central basin from the west coast of India during this time (McCreary et al. 1993).

b. Winter monsoon

Responding to the weak northeasterly winds, the surface Ekman drift in the basin is generally directed westward (Fig. 6a). Total surface currents (sum of Ekman and geostrophic currents) for February are shown in Fig. 6b. The poleward flowing WICC becomes weaker as it moves toward higher latitudes, though this current is less evident in Fig. 6d. Figure 11 represents the surface salinity distribution for the period November–February. The transport of low-salinity water from the BOB to the SEAS by the North Equatorial Current (NEC) and from the SEAS to the northeastern basin by the WICC is well depicted in Fig. 11. The WICC flows poleward against weak local winds (Cutler and Swallow 1984; Shetye et al. 1991; McCreary et al. 1993). McCreary et al. (1993) reported the role of propagating Kelvin waves in driving the WICC. Downwelling coastal Kelvin wave packets, generated by the collapse of the summer monsoon winds in the northern BOB, force a current that brings low-salinity water from the BOB to the SEAS in November–February. They also trigger downwelling Rossby waves along the west coast of India; these waves propagate westward and cross the SEAS. Presence of the low-salinity water in the surface layer of the eastern AS over the high-salinity local water generates a strong stratified layer, as shown in Fig. 1. The saline stratified surface layer shoals the MLD in this region (Fig. 8). However, the propagating downwelling Kelvin wave deepens the ILD to nearly 100 m (Fig. 9). Thus, the shallow MLD and deep ILD cause a thick BL (20–50 m) in the southeastern AS (Fig. 5). Although these forcings are sustained only until February, a thick remnant BL is seen even in March (Fig. 5).

As seen in Fig. 4 and reported by many authors (Thadathil and Gosh 1992; Durand et al. 2004; Shankar et al. 2004; Gopalakrishna et al. 2005; Kurian and Vinayachandran 2006; and Thompson et al. 2006), surface layer temperature inversion is a salient feature of the BL seen in the SEAS. Durand et al. (2007) depict the formation mechanism of the BL and inversion in the SEAS using an OGCM. They concluded that the transport of the merged flow [East India Coastal Current (EICC), winter monsoon current (WMC)] and the recirculation within the SEAS] of low salinity and low SST [due to surface cooling (Luis and Kawamura 2002a,b)] over the downwelled high-salinity local water was the formation mechanism for the observed BL.

The presence of a thick BL (20–50 m) in the northeastern basin during January–February is seen in Fig. 5. During the winter monsoon, the poleward-flowing WICC (Shetye et al. 1991; McCreary et al. 1993) carries low-salinity water from the BOB to the northeastern

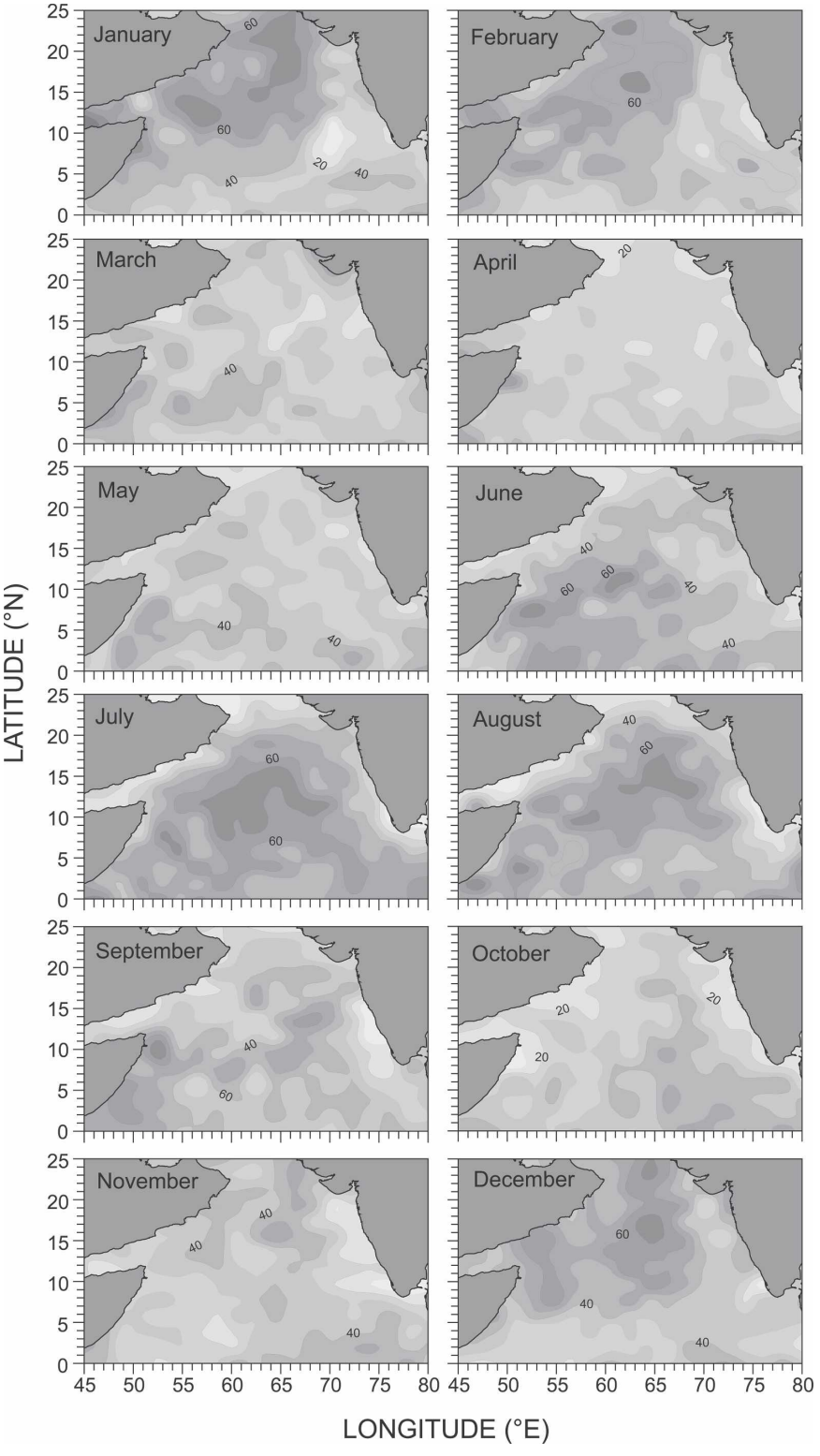

FIG. 8. Seasonal distribution of MLD (m), contour interval: 10 m.

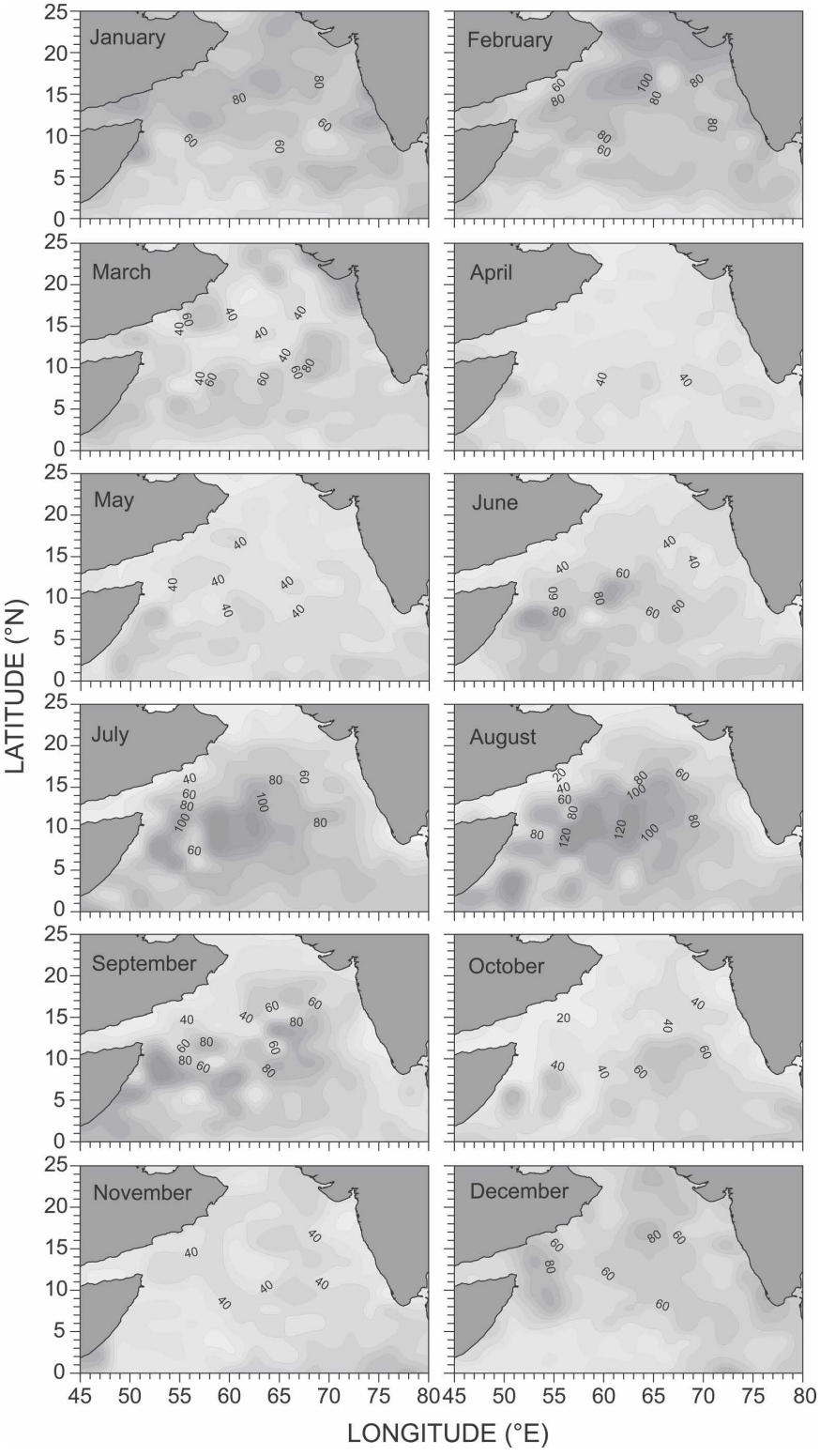

FIG. 9. As in Fig. 8, but for ILD.

AS where it blankets the subsurface ASHSW. Doe (1965) observed strong haline stratification off Karachi, Pakistan, during January, and Banse (1968) reported the occurrence of a near-surface temperature inversion in this region during January–February. Although the ASHSW forms in the surface during November, the ASHSW core is subducted to 50–60 m and moves toward the northeastern boundary by January–February (Kumar and Prasad 1999). Thus, the subsurface ASHSW and the surface low-salinity WICC water lead to a stratified upper layer. During this time, as shown in Fig. 7a, the negative wind stress curl intensifies in this region to deepen the ILD there. The haline stratification shoals the MLD and the downwelling Kelvin wave and negative wind stress curl deepen the ILD to form the observed thick BL.

5. Summary and conclusions

This study provides a detailed description of the seasonal variation of the BLT in the Arabian Sea using historical hydrographic (*WOA-2001* and IODC archives) and recent Argo data. The seasonal variability of the BLT is closely related to the oceanic processes that occur during summer and winter monsoons. During both seasons, the Ekman drift and distribution of low-salinity waters in the surface layer and subduction of ASHSW are the dominant influence on the observed BLT distributions. In addition, the coastal Kelvin waves and the westward-propagating Rossby waves also modulate the observed BLT in the eastern and central AS.

For clarity in understanding these processes schematics showing the monsoonal forcing and other important processes are presented in this section. Figure 12b shows a schematic of the forcing mechanisms for the observed distribution of BLT during the summer monsoon. The summer monsoon facilitates the following major processes in the AS that affect the distribution of the BLT.

During the summer monsoon, a divergence zone occurs north of the maximum wind axis (Findlater jet) and a convergence zone south of it. In the region of Ekman divergence, the effect of turbulent mixing by strong monsoon winds in deepening the MLD/ILD is mitigated by the shoaling effect of upwelling. In contrast, Ekman pumping in the convergence zone promotes the MLD/ILD deepening along with the turbulent mixing by strong winds. The Somali Current carries a wide band of low-salinity water from the equator and dumps it in the Ekman convergence zone. The offshore advection of low-salinity water from upwelling regions also contributes to the surface freshening. During this period the ASHSW, which is formed and subducted in the northern AS (north of 15°N) during winter, spreads toward the equator as a subsurface salinity maximum. The presence of this salinity maximum (ASHSW) and the overlying equatorial low-salinity water (carried by

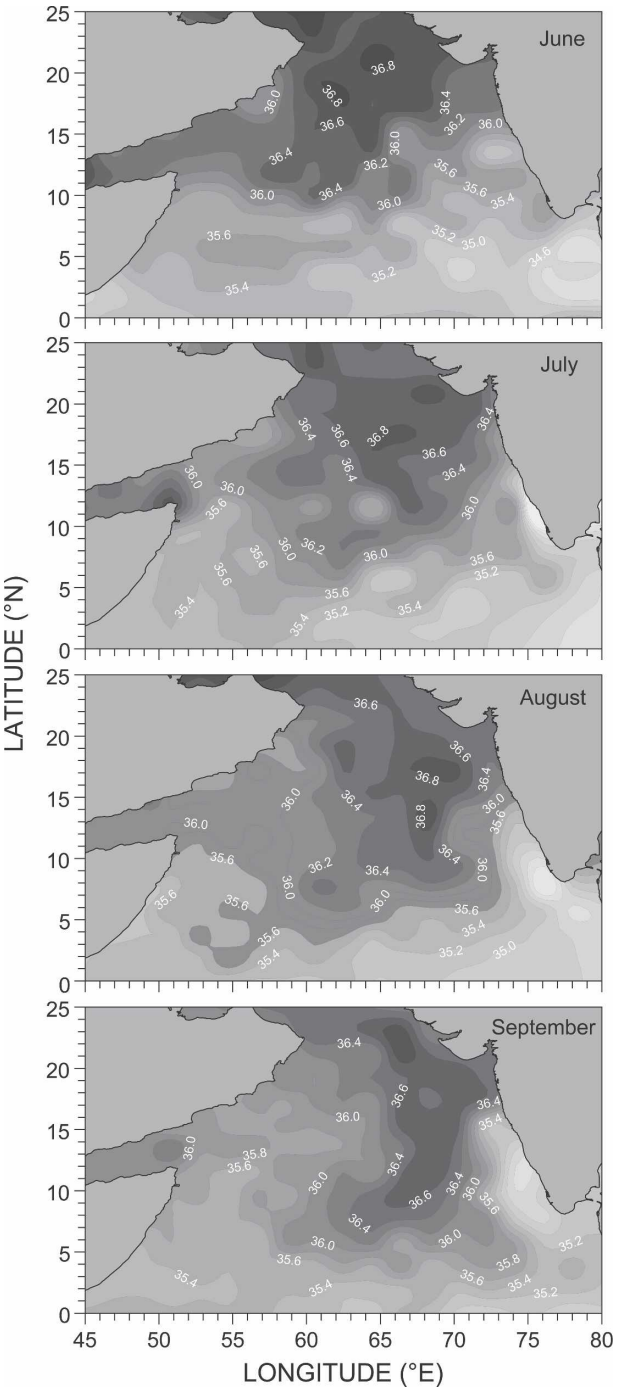

FIG. 10. Distribution of sea surface salinity in the Arabian Sea during the summer monsoon. Contour interval is 0.1 for SSS greater than 35 psu, label shown for 0.2; for SSS less than 35 psu the contour interval is 0.4 psu.

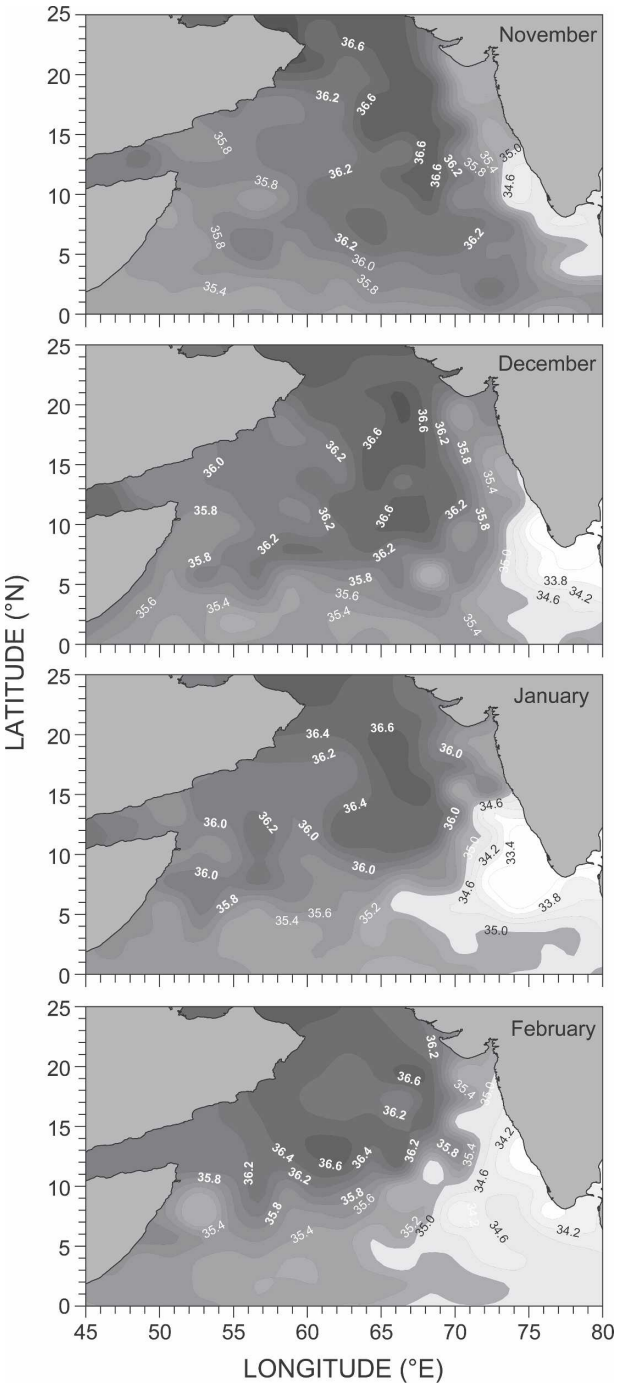

FIG. 11. As in Fig. 10, but for the winter monsoon.

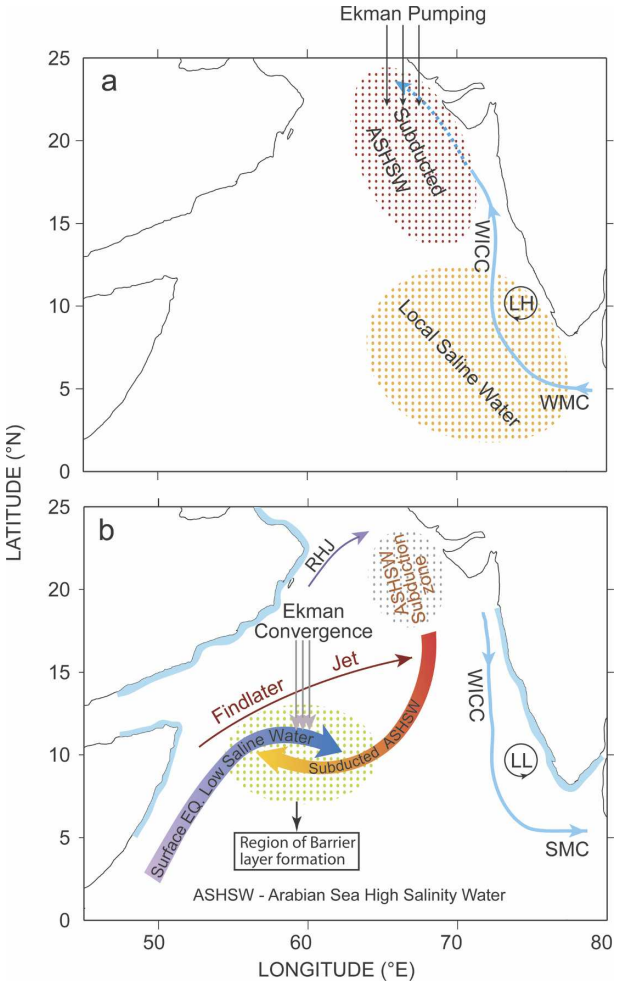

FIG. 12. Schematic of the forcing mechanisms explaining the variability of ILD, MLD, and BLT during (a) January–March and (b) June–September. The red looping arrow shows the southward spreading of the ASHSW being formed and subducted during winter in the region north of 15°N; blue shades along the coast indicate upwelling zones.

the Somali Current) together facilitate the haline stratification that is sufficient to develop the observed BLT in this region during summer.

During winter (November–February), the winds reverse from southwesterly to northeasterly. A schematic of the forcing mechanisms for the observed BLT in the SEAS and in the northeastern basin is shown in Fig. 12a. The WMC off the southern Indian tip is a unified current from the eastern Indian Ocean and the EICC. One branch of the WMC flows around the Laccadive high (LH) and flows poleward as the WICC. Thus, these two currents (WMC and WICC) carry low-salinity water from the head and southern bay into the SEAS and farther to the northeastern basin. Off the southern Indian peninsula, the waters are cooled (due to wind-driven evaporation) by the strong gap (because of the topography of the southern Indian peninsula and Sri Lanka) winds of the northeast monsoon. Note also that these winds advect dry continental air masses over the ocean, favoring strong evaporation. In the SEAS, cool freshwater overlying the warm saline local waters facilitates a strong saline stratified layer that is condu-

cive to temperature inversions and a thick BL, as observed in Figs. 4 and 5, respectively. This is the time when downwelling Kelvin and Rossby waves traverse the SEAS and tend to deepen the ILD along the way. Thus, the shallow MLD due to strong haline stratification and weak winds and deep ILD due to the propagating downwelling waves develop the observed thick BL in the SEAS.

In the northeastern Arabian Sea the forcing mechanisms are similar, but more candidates join in the BL forcing, shown schematically in Fig. 12a. The WICC carries low-salinity water into the northeastern basin as an effect of the poleward-propagating downwelling Kelvin wave. By the time the WICC and the Kelvin wave reach this region, the ASHSW subducts to deeper depths and allows less saline WICC waters to occupy the surface layer. Toward the later part of the winter (January–February), the negative wind stress curl intensifies in this region to reinforce the ILD deepening caused by the downwelling Kelvin wave that has propagated through the region earlier. All of these forcings (as shown in Fig. 12a) support formation of the thick BL in this region during January–February.

Acknowledgments. This research work was supported by the Space Application Center through a grant-in-aid project. The Argo data were collected and made freely available by the International Argo Project and the national program (coordinated by Indian National Centre for Ocean Information System) that contributes to it (www.argo.ucsd.edu; www.jcommops.org). Argo is a pilot program of the Global Ocean Observing System. QuikScat data are produced by Remote Sensing Systems and sponsored by the NASA Ocean Vector Winds Science Team. Data are available at www.remss.com. The altimeter products were produced by Ssalto/Ducacs and distributed by Aviso, with support from CNES. The authors thank R. Uchil for the assistance rendered for the preparation of the figures.

REFERENCES

Anderson, S. P., R. A. Weller, and R. B. Lukas, 1996: Surface buoyancy forcing and the mixed layer of the western Pacific warm pool: Observations and 1D model results. *J. Climate,* **9,** 3056–3085.

Ando, K., and M. J. McPhaden, 1997: Variability of surface layer hydrography in the tropical Pacific Ocean. *J. Geophys. Res.,* **102,** 23 063–23 078.

Argo Science Team, 2000: Report of the Argo science team meeting (Argo-2). Southampton Oceanography Centre, Southampton, United Kingdom, 38 pp.

Banse, K., 1968: Hydrography of the Arabian Sea Shelf of India and Pakistan and effects on demersal fishes. *Deep-Sea Res.,* **15,** 45–79.

Bauer, S., G. L. Hitchcock, and D. B. Olson, 1991: Influence of monsoonally-forced Ekman dynamics upon surface layer depth and plankton biomass distribution in the Arabian Sea. *Deep-Sea Res.,* **38,** 531–553.

Chelton, D. B., M. G. Schlax, J. M. Lyman, and G. C. Johnson, 2003: Equatorially trapped Rossby waves in the presence of meridionally sheared baroclinic flow in the Pacific Ocean. *Prog. Oceanogr.,* **56,** 323–380.

Cressie, N. A. C., 1991: *Statistics for Spatial Data.* John Wiley and Sons, 900 pp.

Cutler, A. N., and J. C. Swallow, 1984: Surface currents of the Indian Ocean (to 25°S, 100°E): Compiled from historical data archived by the Met Office. Institute of Oceanographic Sciences Rep. 187, Wormley, United Kingdom, 8 pp+36 charts.

Deutsch, C. V., and A. G. Journel, 1992: *GSLIB-Geostatistical Software Library and User's Guide.* Oxford University Press, 338 pp.

Doe, L. A. E., 1965: Physical conditions on the shelf near Karachi during postmonsoonal calm, 1964. *Ocean Sci. Ocean Eng.,* **1,** 278–292.

Durand, F., S. R. Shetye, J. Vialard, D. Shankar, S. S. C. Shenoi, C. Ethe, and G. Madec, 2004: Impact of temperature inversions on SST evolution in the south-eastern Arabian Sea during the pre-summer monsoon season. *Geophys. Res. Lett.,* **31,** L01305, doi:10.1029/2003GL018906.

——, D. Shankar, C. de Boyer Montégut, S. S. C. Shenoi, B. Blanke, and G. Madec, 2007: Modeling the barrier-layer formation in the southeastern Arabian Sea. *J. Climate,* **20,** 2109–2120.

Findlater, J., 1969: A major low-level air current near the Indian Ocean during the northern summer. *Quart. J. Roy. Meteor. Soc.,* **95,** 362–380.

Gopalakrishna, V. V., Z. Johnson, G. Salgaonkar, K. Nisha, C. K. Rajan, and R. R. Rao, 2005: Observed variability of sea surface salinity and thermal inversions in the Lakshadweep Sea during contrast monsoons. *Geophys. Res. Lett.,* **32,** L18605, doi:10.1029/2005GL023280.

Jerlov, N. G., 1968: *Optical Oceanography.* Elsevier, 199 pp.

Joseph, S., and H. J. Freeland, 2005: Salinity variability in the Arabian Sea. *Geophys. Res. Lett.,* **32,** L09607, doi:10.1029/2005GL022972.

Kara, A. B., P. A. Rochford, and H. E. Hurlburt, 2000: An optimal definition for ocean mixed layer depth. *J. Geophys. Res.,* **105,** 16 803–16 822.

Kurian, J., and P. N. Vinayachandran, 2006: Formation mechanisms of temperature inversions in the southeastern Arabian Sea. *Geophys. Res. Lett.,* **33,** L17611, doi:10.1029/2006GL027280.

Levitus, S., 1998: *Climatological Atlas of the World Ocean.* Tech. Rep. 13, NOAA, Rockville, MD, 166 pp.

Lewis, M. R., M.-E. Carr, G. C. Feldman, W. Esaias, and C. McClain, 1990: Influence of penetrating solar radiation on the heat budget of the equatorial Pacific Ocean. *Nature,* **347,** 543–545.

Luis, A. J., and H. Kawamura, 2002a: Dynamics and mechanism for sea surface cooling near the Indian tip during winter monsoon. *J. Geophys. Res.,* **107,** 3187, doi:10.1029/2000JC000455.

——, and ——, 2002b: A case study of sea surface temperature—Cooling dynamics near the Indian tip during May 1997. *J. Geophys. Res.,* **107,** 3171, doi:10.1029/2000JC000778.

Lukas, R., and E. Lindstrom, 1991: The mixed layer of the western equatorial Pacific Ocean. *J. Geophys. Res.,* **96** (Suppl.), 3343–3358.

Masson, S., P. Delecluse, J.-P. Boulanger, and C. Menkes, 2002: A model study of the seasonal variability and formation mechanisms of the barrier layer in the eastern equatorial Indian Ocean. *J. Geophys. Res.,* **107,** 8017, doi:10.1029/2001JC000832.

McCreary, J. P., P. K. Kundu, and R. L. Molinari, 1993: A numerical investigation of dynamics, thermodynamics and mixed-layer processes in the Indian Ocean. *Prog. Oceanogr.,* **31,** 181–244.

Morrison, J. M., 1997: Inter-monsoonal changes in the *T–S* properties of the near-surface waters of the northern Arabian Sea. *Geophys. Res. Lett.,* **24,** 2553–2556.

Murtugudde, R., and A. J. Busalacchi, 1999: Interannual variability of the dynamics and thermodynamics of the tropical Indian Ocean. *J. Climate,* **12,** 2300–2326.

——, J. P. McCreary, and A. J. Busalacchi, 2000: Oceanic processes associated with anomalous events in the Indian Ocean with relevance to 1997–1998. *J. Geophys. Res.,* **105,** 3295–3306.

Pond, S., and G. L. Pickard, 1983: *Introductory Dynamical Oceanography.* 2nd ed. Pergamon Press, 329 pp.

Prasad, T. G., and M. Ikeda, 2002a: The wintertime water mass formation in the northern Arabian Sea: A model study. *J. Phys. Oceanogr.,* **32,** 1028–1040.

——, and ——, 2002b: A numerical study of the seasonal variability of Arabian Sea high-salinity water. *J. Geophys. Res.,* **107,** 3197, doi:10.1029/2001JC001139.

Prasanna Kumar, S., and T. G. Prasad, 1999: Formation and spreading of Arabian Sea high-salinity water mass. *J. Geophys. Res.,* **104,** 1455–1464.

Qu, T., and G. Meyers, 2005: Seasonal variation of barrier layer in the southeastern tropical Indian Ocean. *J. Geophys. Res.,* **110,** C11003, doi:10.1029/2004JC002816.

Rao, R. R., and R. Sivakumar, 2003: Seasonal variability of sea surface salinity and salt budget of the mixed layer of the north Indian Ocean. *J. Geophys. Res.,* **108,** 3009, doi:10.1029/2001JC000907.

Rochford, D. J., 1964: Salinity maximum in the upper 100 meters of the north Indian Ocean. *Aust. J. Mar. Freshwater Res.,* **15,** 1–24.

Schott, F. A., and J. P. McCreary, 2001: The monsoon circulation of the Indian Ocean. *Prog. Oceanogr.,* **51,** 1–123.

Shankar, D., P. N. Vinayachandran, and A. S. Unnikrishnan, 2002: The monsoon currents in the north Indian Ocean. *Prog. Oceanogr.,* **52,** 63–120.

——, and Coauthors, 2004: Observational evidence for westward propagation of temperature inversions in the southeastern Arabian Sea. *Geophys. Res. Lett.,* **31,** L08305, doi:10.1029/2004GL019652.

Shenoi, S. S. C., S. R. Shetye, A. D. Gouveia, and G. S. Michael, 1993: Salinity extrema in the Arabian Sea. *Monsoon Biogeochemistry,* V. Ittekkot and R. R. Nair, Eds., Im Selbstverlag des Geologisch-Paläontologischen Institutes der Universität Hamburg, 37–39.

——, D. Shankar, and S. R. Shetye, 2004: Remote forcing annihilates barrier layer in southeastern Arabian Sea. *Geophys. Res. Lett.,* **31,** L05307, doi:10.1029/2003GL019270.

Shetye, S. R., A. D. Gouveia, S. S. C. Shenoi, G. S. Michael, D. Sundar, A. M. Almeida, and K. Santanam, 1991: The coastal current off western India during the northeast monsoon. *Deep-Sea Res.,* **38A,** 1517–1529.

Sprintall, J., and M. Tomczak, 1992: Evidence of the barrier layer in the surface layer of the tropics. *J. Geophys. Res.,* **97,** 7305–7316.

Thadathil, P., and A. K. Ghosh, 1992: Surface layer temperature inversion in the Arabian Sea during winter. *J. Oceanogr.,* **48,** 293–304.

——, and P. M. Muraleedharan, 2004: Validation of ARGO data from the Indian Ocean, Gayana (2004). *Int. J. Biodiversity Oceanol. Conserv.,* **68,** 456–458.

——, V. V. Gopalakrishna, P. M. Muraleedharan, G. V. Reddy, N. Araligidad, and S. Shenoy, 2002: Surface layer temperature inversion in the Bay of Bengal. *Deep-Sea Res. I,* **49,** 1801–1818.

——, P. M. Muraleedharan, R. R. Rao, Y. K. Somayajulu, G. V. Reddy, and C. Revichandran, 2007: Observed seasonal variability of barrier layer in the Bay of Bengal. *J. Geophys. Res.,* **112,** C02009, doi:10.1029/2006JC003651.

Thompson, B., C. Gnanseelan, and P. S. Salvekar, 2006: Seasonal evolution of temperature inversions in the north Indian Ocean. *Curr. Sci.,* **90,** 697–704.

Tomczak, M., 1995: Salinity variability in the surface layer of the tropical western Pacific Ocean. *J. Geophys. Res.,* **100,** 20 499–20 516.

Vialard, J., and P. Delecluse, 1998a: An OGCM study for the TOGA decade. Part I: Role of salinity in the physics of the western Pacific fresh pool. *J. Phys. Oceanogr.,* **28,** 1071–1088.

——, and ——, 1998b: An OGCM study for the TOGA decade. Part II: Barrier-layer formation and variability. *J. Phys. Oceanogr.,* **28,** 1089–1106.

Vinayachandran, P. N., V. S. N. Murty, and V. Ramesh Babu, 2002: Observations of barrier layer formation in the Bay of Bengal during summer monsoon. *J. Geophys. Res.,* **107,** 8018, doi:10.1029/2001JC000831.

Wyrtki, K., 1971: *Oceanographic Atlas of the International Indian Ocean Expedition.* U.S. Government Printing Office, 531 pp.

You, Y., 1995: A rain formed barrier layer model. *Ocean Modelling,* **106,** 3–8.

CORRIGENDUM

It has come to our attention that a coauthor's name was misspelled in "Seasonal Variability of the Observed Barrier Layer in the Arabian Sea," by Thadathil et al., which appeared in the *Journal of Physical Oceanography*, Vol. 38, No. 3, 624–638. The seventh coauthor listed on this paper's title page should be Raghu Murtugudde.

The staff of the *Journal of Physical Oceanography* regrets any inconvenience this error may have caused.